

Numerical Simulation of the Seasonal Variation of Mesospheric Water Vapor

ANNE K. SMITH

*Space Physics Research Laboratory, Department of Atmospheric, Oceanic and Space Sciences
University of Michigan, Ann Arbor, Michigan*

GUY P. BRASSEUR

National Center for Atmospheric Research, Boulder, Colorado

A two-dimensional radiative/dynamical/chemical model is used to investigate the role of varying vertical diffusivity on the distribution and temporal variability of water vapor in the mesosphere. Model runs in which the effective turbulent Prandtl number varies over 2 orders of magnitude (values of 1, 10, and 100) are compared. The results indicate that a Prandtl number of 10 or more gives a simulation of mesospheric water vapor characterized by a strong decrease with height and a seasonal cycle with maximum mixing ratios during late summer. The test with a small Prandtl number gives, in contrast, very weak vertical gradients of concentration and a semiannual cycle with maxima in late winter and late summer. The very high Prandtl number case was included to test the role of vertical diffusion in the model when the effective diffusivity coefficient is very small. Comparison of these three cases indicates that the vertical structure of water is sensitive to the effective diffusivity over the range tested. The results also indicate that meridional advection by the mean circulation has a significant influence on the vertical distribution of water in the mesosphere.

1. INTRODUCTION

Water vapor in the mesosphere is important for its role in chemistry and also as one of several proxy indicators of dynamical motion. The ozone budget in the mesosphere is, to a large extent, determined by the abundance of water vapor. Water is injected into the middle atmosphere from the troposphere, primarily in the tropics, and is also produced by the oxidation of methane. This latter process produces a maximum in the H₂O mixing ratio of about 5-7 ppmv near the stratopause [Gille and Russell, 1984].

The water molecule is relatively impervious to chemical destruction below approximately 70 km altitude. Above this level, it can be easily photolyzed by solar Lyman α radiation (121.6 nm). The net effect of this photolysis and the ensuing chemical reactions of the products is the conversion of a fraction of water vapor into molecular and atomic hydrogen. In the thermosphere the hydrogen atom becomes so nonreactive that it may be transported to higher altitudes and eventually escape to space.

As a result of these photochemical processes, H₂O exhibits a strong vertical gradient in the mesosphere. The photolysis coefficient of H₂O at 70 km is of the order of 10⁻⁶ s⁻¹; thus at this altitude the photochemical lifetime is about 10 days. Since the chemical lifetime of H₂O is similar to the characteristic time for vertical transport, water vapor is an excellent indicator of vertical exchanges in this region of the atmosphere.

There is continuing debate about the role of dynamical transport in controlling the distribution of water vapor in the mesosphere. A study addressing this issue was performed by

Garcia and Solomon [1985], using a two-dimensional dynamical/chemical model of the middle atmosphere. They adapted the parameterized representation of wave breaking developed by *Lindzen [1981]* and looked at the water vapor distribution as one measure of the effect that gravity waves have on the temporal variability of chemical constituents. They attributed the semiannual variability of H₂O in the model mesosphere to variations in vertical diffusion. The temporal variations in H₂O then give rise, through chemistry, to an out-of-phase semiannual variation in ozone, which has been observed in Solar Mesosphere Explorer (SME) data [Thomas *et al.*, 1984]. Their conclusions are different from those reached by *Holton and Schoeberl [1988]* in another modeling study. In their model, which also uses a version of the *Lindzen [1981]* parameterization, H₂O is more sensitive to advection by the mean meridional circulation than to gravity wave or turbulent transport. They use the argument that the diffusion should be weaker than that derived by *Lindzen [1981]* and used by *Garcia and Solomon [1985]*, because localization of turbulence makes the effective Prandtl number greater than unity. However, in *Holton and Schoeberl's [1988]* model, even strong diffusion ($Pr=1$, as in works by *Lindzen [1981]* and *Garcia and Solomon [1985]*) gave a water vapor distribution that was advectively controlled. An argument against control by diffusion comes from ground-based measurements of mesospheric water vapor [Bevilacqua *et al.*, 1989] that indicate that H₂O at 40°N has primarily an annual cycle, although there is a suggestion in the data of a weak semiannual component. The one-dimensional model of *Bevilacqua et al. [1990]* indicates that the observed gradient in mesospheric water vapor is not compatible with diffusion as large as that used by *Garcia and Solomon [1985]*.

Our two-dimensional model is formulated in a way that is basically similar to that of *Garcia and Solomon [1985]*. The results of some experiments with this model can give an idea of why the analyses of *Garcia and Solomon [1985]* and *Holton and*

Copyright 1991 by the American Geophysical Union.

Paper number 91JD00226.
0148-0227/91JD-00226\$05.00

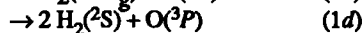
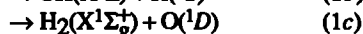
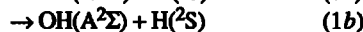
Schoeberl [1988] give different answers and how those answers fit with the observed H₂O variations.

2. MODEL DESCRIPTION

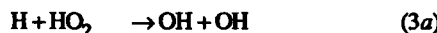
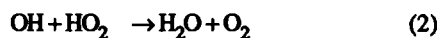
The model used in this study is zonally averaged and global in domain and extends from the Earth's surface to approximately 85 km (the vertical coordinate is log pressure). The dynamical formulation is based on the quasi-geostrophic transformed mean system of equations [Andrews and McIntyre, 1976], with parameterizations for Rossby wave [Hitchman and Brasseur, 1988] and gravity wave [Lindzen, 1981; Brasseur and Hitchman, 1987] interactions. The diabatic forcing is computed from the radiative algorithm developed for the National Center for Atmospheric Research (NCAR) community climate model [Kiehl et al., 1987] up to 65 km and is parameterized above that level. Chemical reactions among the oxygen, nitrogen, hydrogen, carbon, chlorine, bromine, and sulfur groups are included. Reaction rates and cross sections are taken from DeMore [1987]. A full description of the model is given by Brasseur et al. [1990].

Since the upper boundary is located at 85 km near the mesopause, the impact of the boundary conditions on mesospheric water vapor has been evaluated. Tests varying the magnitude and type (i.e., flux versus specified mixing ratio) of the H₂O boundary condition change the H₂O and O₃ mixing ratio near the boundary but have only a minor effect on the results at and below 75 km, leading us to the conclusion that the boundary is not seriously distorting the findings. An upward flux of water at 85 km was used for these cases.

There are still some major uncertainties concerning the odd hydrogen chemistry in the mesosphere. Above about 70 km, H₂O is photolyzed by solar radiation, primarily at Lyman α (121.6 nm) and in the O₂ Schumann-Runge bands (175-200 nm). In the latter case the products of the photodissociation are OH(X² Π) and H(²S), but in the region of Lyman α several different paths have to be considered.



The relative efficiency of the different paths involved is very uncertain, but it is believed that the dominant path leads to H atoms and OH radicals [Nicolet, 1978, 1989]. The hydrogen radicals (H, OH) resulting from water photolysis are in part converted to HO₂ and can recombine to produce either H₂O or H₂.



Several possible branching ratios are given by DeMore et al. [1987]. We adopt those from a study by Keyser et al. [1985], giving 90% for (3a), 2% for (3b), and 8% for (3c). Reactions (3c) and (1c) are both sources of molecular hydrogen in the mesosphere.

3. WATER VAPOR BUDGET CALCULATIONS

The continuity equation for H₂O is

$$\frac{\partial \bar{\mu}}{\partial t} = -\bar{v}^* \frac{\partial \bar{\mu}}{\partial y} - \bar{w}^* \frac{\partial \bar{\mu}}{\partial z} + \bar{P} - \bar{L}\bar{\mu} + \frac{1}{\cos\phi} \frac{\partial}{\partial y} \left(\cos\phi K_{yy} \frac{\partial \bar{\mu}}{\partial y} \right) + \frac{1}{\rho_0} \frac{\partial}{\partial z} \left(\rho_0 K_{zz} \frac{\partial \bar{\mu}}{\partial z} \right) \quad (4)$$

The symbols are defined as

$\bar{\mu}$	zonal mean mixing ratio;
\bar{v}^*, \bar{w}^*	meridional and vertical residual mean velocity;
\bar{P}	zonal mean photochemical production;
\bar{L}	zonal mean photochemical loss coefficient;
K_{yy}	meridional eddy transport coefficient;
D	parameterized vertical diffusion coefficient;
Pr	effective turbulent Prandtl number;
$K_{zz} (= D/Pr)$	net vertical eddy transport coefficient.

The meridional eddy transport coefficient K_{yy} is determined from the parameterization of Hitchman and Brasseur [1988] and has only a small effect on the water vapor budget in the mesosphere. D is determined from the Lindzen parameterization, as adapted by Brasseur and Hitchman [1987]. There are several theoretical studies suggesting that the Prandtl number Pr should be significantly greater than 1 [Chao and Schoeberl, 1984; Fritts and Dunkerton, 1985; Coy and Fritts, 1988; Schoeberl, 1988]; estimated values range from 3 to 10 and may be even larger. This is also supported by observations of the thermal structure [Strobel et al., 1985] and trace species distributions [Strobel et al., 1987; Brasseur and Offermann, 1986; Allen et al., 1981; Bevilacqua et al., 1990]. Results are presented for three cases: $Pr=1$, $Pr=10$, and $Pr=100$. The first, which derives from the assumption that dissipation acting on breaking gravity waves is in the form of uniformly distributed turbulence, is comparable to that used by Garcia and Solomon [1985]. $Pr=10$ is near the high end of theoretical estimates but is not outside of the normal range. $Pr=100$ is higher than theoretical studies would suggest but is included to evaluate the balance achieved in the model when the effective vertical diffusion coefficient is very small. In a given run the same value of Pr is used for temperature and for all transported chemical families and species. Two additional runs, described in section 4, were included to supplement the comparison of the model results with microwave measurements.

The direct role of Pr in the water vapor budget is clear from (4); for a given vertical gradient a Pr of 10 means that vertical transport induced by gravity waves is only 10% of what it is in the $Pr=1$ case. The indirect effects are less obvious but can also be important. The mean circulation can respond to a change in diffusion either through dynamical feedbacks (for example, weaker heat diffusion changes the thermal field, which in turn leads to a different mean meridional circulation) or through chemical feedbacks (for example, changes in diffusion lead to changes in the distribution of radiatively active gases, and the resulting modifications in diabatic heating give a different thermal field). There is also the potential for chemical feedbacks directly on H₂O, since both \bar{P} and \bar{L} in (4) depend on the concentrations of other species with which H₂O interacts. For example, H₂O molecules are formed from the destruction of methane, which is produced at the Earth's surface [e.g., Jones et al., 1986; Le Texier et al., 1988]. Weaker diffusion results in slower upward transport of methane into the mesosphere and can therefore lead to a redistribution in the region of H₂O

production. Examination of the fields generated by these three runs indicate that there are indeed differences in \bar{v}^* , \bar{w}^* , \bar{P} and \bar{L} , but that these are small compared to the changes in H_2O due directly to Pr .

In their conceptual analysis, *Holton and Schoeberl* [1988] assumed that the vertical structure of water could be represented by the vertical scale height h_s , satisfying $(\partial\bar{\mu}/\partial z) = -\bar{\mu}/h_s$. Using this definition, but without making a priori assumptions about advective or diffusive control of h_s , we can determine the steady state scale height from (4). The assumptions are made that photochemical production is negligible (valid in the mesosphere) and that no significant time tendency results from the meridional eddy transport (K_{yy}). Both of these assumptions have been verified by budget studies conducted with the model. Then (4) can be written in terms of scale height as

$$-\bar{v}^* \frac{\partial\bar{\mu}}{\partial y} + \bar{w}^* \frac{\bar{\mu}}{h_s} - \bar{L}\bar{\mu} + \frac{K_{zz}}{h_s^2} \bar{\mu} - \left(\frac{\partial K_{zz}}{\partial z} - \frac{K_{zz}}{H} \right) \frac{\bar{\mu}}{h_s} = 0, \quad (5)$$

A heuristic representation of the limiting cases for advective and diffusive control was given by *Bevilacqua et al.* [1990] and is consistent with the analysis of *Holton and Schoeberl* [1988]. They consider, for a given H_2O scale height h_s , the effect of domination by one or the other of two transport processes, advection by the mean vertical wind, and vertical diffusion. H_2O decreases with height in the mesosphere, giving a positive h_s . Vertical diffusion transports air with higher H_2O mixing ratio upward from the lower mesosphere and gives a positive tendency that peaks during the twice-yearly maxima in K_{zz} . Mean vertical advection gives a negative tendency during winter and a positive one during summer. For a decrease of water vapor mixing ratio with height, as occurs in the majority of observations, mean vertical advection will tend to induce an annual cycle with a maximum mixing ratio in late summer, while vertical diffusion will tend to produce two maxima during late winter and late summer. This expected temporal cycle is used to argue that, in order to be consistent with ground-based observations [*Bevilacqua et al.*, 1989, 1990], advection by the mean circulation must be more important than diffusion in determining the seasonal variations of water in the mesosphere. This argument depends somewhat on water having a fairly strong decrease with height in the upper mesosphere, as is indicated by observations and simple photochemical theory. However, that structure can itself depend on the transport.

In general, a steady state at any given time can be attained only if there is at least one process that is decreasing and one that is increasing the H_2O mixing ratio, or if the tendencies of all processes are zero. This means, for example, that a balance cannot be attained by diffusion and mean vertical advection during the summer; an effective loss due either to photochemistry or to meridional advection is also necessary. Diffusion and photochemical loss have opposing tendencies, which suggests that they could be in approximate balance during all seasons, as long as L is not zero. This is, in fact, the formulation of most one dimensional models [e.g., *Strobel et al.*, 1985; *Allen et al.*, 1981], particularly those that represent the global mean atmosphere. However, during the winter solstice the photochemical loss rate is small but the diffusive transport coefficient (K_{zz}) is near its maximum, so on a local scale a balance between the two does not occur.

Equation (5) can be solved for scale height, giving

$$h_s = \left[2 \left(L + \frac{\bar{v}^* \partial\bar{\mu}}{\bar{\mu} \partial y} \right) \right]^{-1} \left\{ - \left(\frac{\partial K_{zz}}{\partial z} - \frac{K_{zz}}{H} - \bar{w}^* \right) \pm \sqrt{\left(\frac{\partial K_{zz}}{\partial z} - \frac{K_{zz}}{H} - \bar{w}^* \right)^2 + 4 \left(L + \frac{\bar{v}^* \partial\bar{\mu}}{\bar{\mu} \partial y} \right) K_{zz}} \right\} \quad (6)$$

L and K_{zz} are by definition nonnegative; if $[L + (\bar{v}^*/\bar{\mu})/(\partial\bar{\mu}/\partial y)]$ is positive, there is always at least one nonnegative solution, so that a steady state is possible under both summer and winter conditions. In the cases examined here, advection by the mean meridional flow is often a dominant effect and for some regions no real solution to (6) exists. Lack of a real solution indicates that the H_2O vertical structure cannot be represented by a scale height or that the distribution will not reach a steady state. Presence of a solution indicates that it is possible to reach a steady state under extant conditions but is not sufficient to indicate that the actual vertical structure is near its steady state value.

Consider the case in which the H_2O tendency due to diffusion is dominated by the direct diffusive contribution $K_{zz}(\partial^2\bar{\mu}/\partial z^2)$ rather than the contribution from the vertical structure of the density weighted diffusion $-(\partial K_{zz}/\partial z - K_{zz}/H)(\partial\bar{\mu}/\partial z)$. There is negative feedback associated with this vertical diffusion and the vertical structure of the trace species. Therefore, the change in tendency due to diffusion will be reduced over what it would be were the vertical structure of tracer fixed. In the one-dimensional modeling case (all advection neglected) a steady state is maintained when

$$-\bar{L}\bar{\mu} + \frac{K_{zz}}{h_s^2} \bar{\mu} = 0$$

$$h_s = \sqrt{\frac{K_{zz}}{L}} = \sqrt{\frac{1}{Pr}} \cdot \sqrt{\frac{D}{L}} \quad (7)$$

In this special case the steady state value of K_{zz}/h_s^2 does not change when Pr varies. An increase in Pr results in a shift in the vertical distribution of tracer, as represented by h_s , so that the diffusion is always exactly sufficient to balance the loss rate. Significant changes in K_{zz} must be accompanied by changes in the vertical structure of water vapor but will have no impact on the relative importance of the diffusive tendency in the overall water vapor budget. This negative feedback mechanism can still be important when the advective tendencies from (6) are also considered. Vertical advection by the mean meridional circulation will influence this feedback since it both depends on, and contributes to, the vertical structure.

4. RESULTS

In this section we present results from the three model runs that are relevant to the issue of the role of vertical diffusion in the control of mesospheric water vapor. Figure 1 shows the annual evolution at a pressure surface near 75 km of mean meridional motion \bar{v}^* , mean vertical motion \bar{w}^* , and eddy diffusion K_{zz} for the intermediate Prandtl number ($Pr=10$) case. The other two model runs (not shown) have \bar{v}^* and \bar{w}^* values that are quite similar to the $Pr=10$ case and K_{zz} values that differ by an amount approximately proportional to the inverse

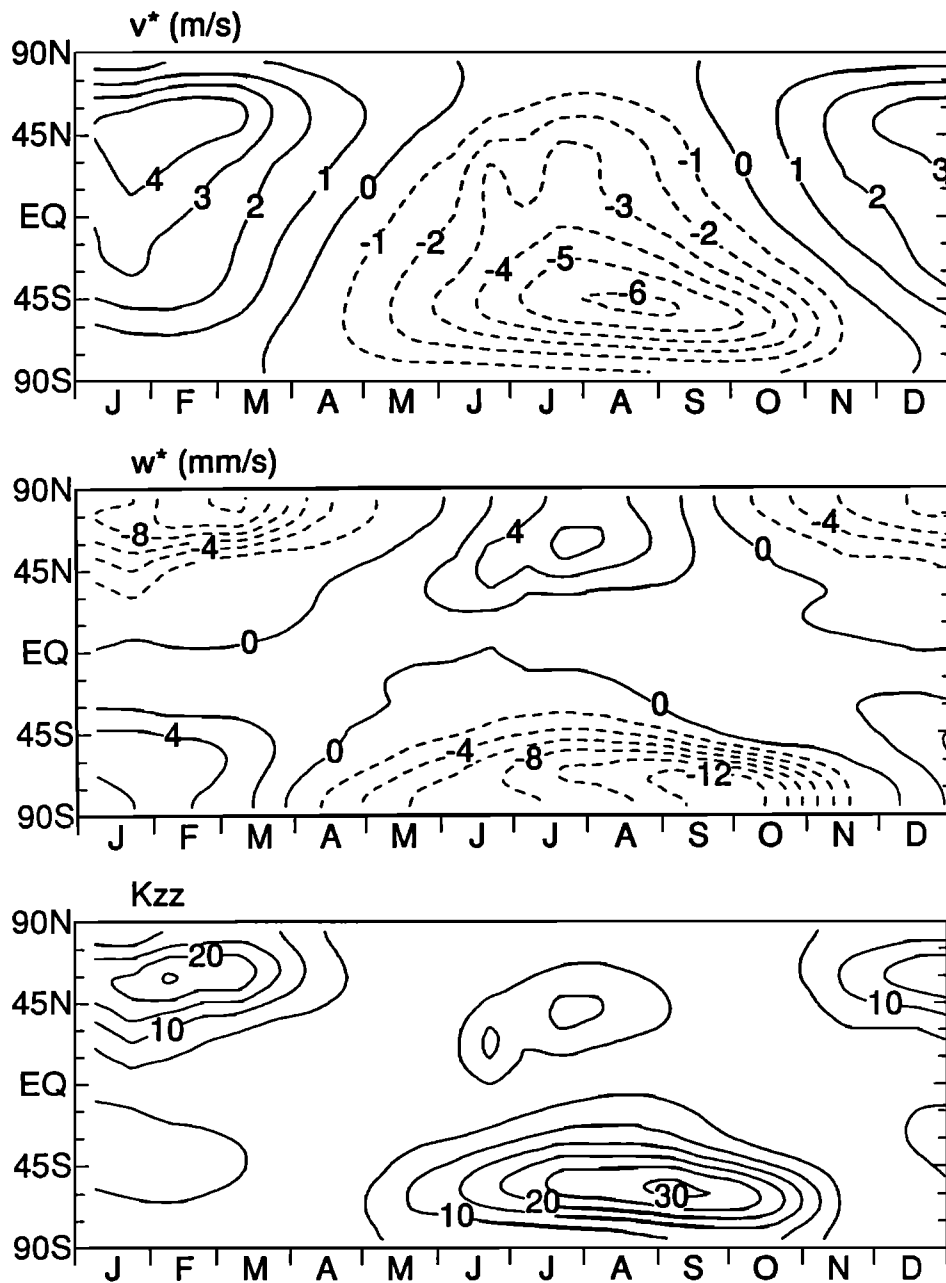


Fig. 1. Mean meridional velocity (top; units are m s^{-1}), mean vertical velocity (center; units are mm s^{-1}) and net vertical diffusion rate (bottom; units are m s^{-1}) plotted versus latitude and time for one model year on a constant pressure surface at approximately 75 km. Values are from the model run with $Pr=10$.

Prandtl numbers. Both the mean circulation and K_{zz} have a large annual cycle (largest magnitudes between the winter solstice and the spring equinox), and K_{zz} has secondary maxima at the summer solstices, giving a semiannual component as well.

The time histories of H_2O mixing ratios at this level for the three model runs are shown in Figure 2. In the $Pr=1$ case the water is dominated by a semiannual variation with peaks after the solstices, whereas in the $Pr=10$ and $Pr=100$ cases a single maximum between the summer solstice and the autumnal equinox is evident in both hemispheres. The annual components of the cycles in water are in phase in the three figures. These comparisons point to the large diffusion coefficient as being responsible for the semiannual variation

in water vapor concentration in the small Prandtl number case, in support of the findings of Garcia and Solomon [1985]. (Their results have largest H_2O concentrations at the solstices, rather than 1-2 months afterwards.) Another way in which a semiannual cycle can be induced from the model wind fields is through meridional advection across the equator by the mean flow. This could account for the weak semiannual variation apparent in low latitudes in Figure 2b, which appears to result from a tropical extension of the late winter peak in H_2O mixing ratio from both hemispheres, which was also noted by Holton and Schoeberl [1988]. However, meridional advection would not be likely to produce the distinct maxima, separated by low values in the subtropical spring, seen in the distribution of H_2O from the high diffusion case (Figure 2a).

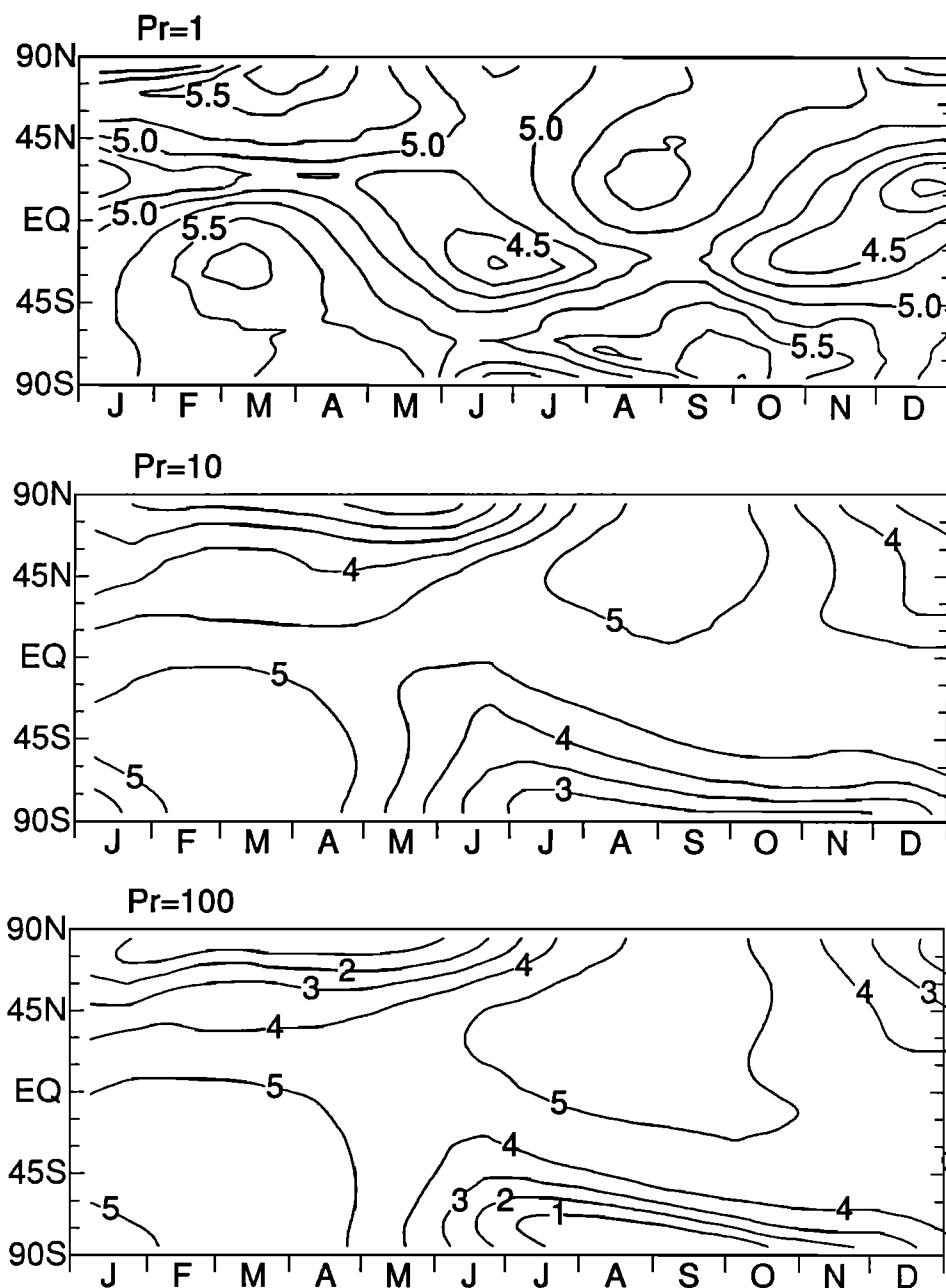


Fig. 2. H_2O mixing ratio (ppmv) for the model runs with $Pr=1$ (top), $Pr=10$ (center), and $Pr=100$ (bottom), plotted versus latitude and time for one model year on a constant pressure surface at approximately 75 km. Contour interval is 0.25 ppmv for the top panel, 0.5 ppmv for the center panel, and 1 for the bottom panel.

Although the $Pr=1$ case supports the conclusion of Garcia and Solomon [1985] that temporal variability in H_2O results from variations in diffusion, there are a number of differences between the water distributions in our model study and theirs. Profiles presented by Le Texier *et al.* [1988], obtained from the Garcia and Solomon [1985] model, show much larger mesospheric water mixing ratios in summer than in winter, whereas in our $Pr=1$ case the differences are small. Their maximum H_2O occurred near the time of the solstices [Garcia and Solomon, 1985], and ours occurred 1-2 months later. These differences are most likely a result of differences in the models' K_{zz} profiles. Our $Pr=1$ model run has substantially larger K_{zz} [Brasseur and Hitchman, 1987] in the lower

mesosphere than the values shown by Garcia and Solomon [1985], and our maxima occur midway between the solstices and equinoxes, rather than at the solstices as theirs do. Our simulation has largest K_{zz} values during the winter, while theirs reach a maximum in the summer. When these differences in K_{zz} between our model and that used by Garcia and Solomon [1985] and Le Texier *et al.* [1988] are taken into account, we see that in both simulations larger water mixing ratios in the upper mesosphere are correlated with larger values of K_{zz} .

These features of the present model's K_{zz} profiles are highly dependent on factors that are controlled from outside the mesosphere. The altitude at which K_{zz} reaches its maximum depends primarily on the effective amplitude of the

parameterized gravity wave at the tropopause. For larger effective amplitudes, the waves break, and generate mixing, at lower altitudes. The effective amplitude is specified in the model, and was selected so that the gravity wave drag in the model corresponded to that derived from Limb Infrared Monitor of the Stratosphere (LIMS) observations [Brasseur and Hitchman, 1987], which extend through the lower part of the mesosphere.

The temporal variability of K_{zz} , as of gravity wave momentum deposition, is controlled by the temporal variations in the transmissivity of the atmosphere below the mesosphere to gravity waves. The model has a tendency to delay the transition from winter westerlies to summer easterlies in the stratosphere compared to that observed for the Northern Hemisphere. This is likely to be a result of the way planetary wave drag is treated in the model [Hitchman and Brasseur, 1987] and may indicate insufficient drag in late winter and spring of the Northern Hemisphere. In the Southern Hemisphere, the usual time for the switch from westerlies to easterlies is relatively later and corresponds well to the model timing.

The present study focuses on understanding how water vapor variations are related to K_{zz} variations, not on determining the "correct" values of K_{zz} . In fact, the extent to which transport can be represented by a diffusion coefficient is itself open to question. For our goal it is important to know that there are uncertainties in the temporal and spatial distribution of K_{zz} , and of \bar{v}^* and \bar{w}^* , that can affect the distribution and variability of trace species. The possible sources outlined here for the difference between our model and that of Garcia and Solomon [1985] should be considered in comparing the results of our model with theirs, as well as with other models and with observations. However, these uncertainties in the distribution of K_{zz} do not invalidate the basic finding concerning the relationship of water vapor variability to the magnitude of the Prandtl number.

The relative magnitudes of the contributions to H_2O tendency in January for the three model runs are shown in Figure 3, calculated from (4). Four curves are shown: mean vertical advection, mean meridional advection, vertical diffusive transport, and photochemical production and loss. Meridional eddy transport and the net time tendency are both small and are omitted. In all model runs an approximate balance is indicated, consistent with the moderate rate of change of H_2O mixing ratio with time (Figure 2). The photochemical production/loss terms have similar magnitude and meridional variation in the two cases; the differences primarily reflect the differences in H_2O rather than in the loss coefficients L , in the different cases. The tendencies due to diffusive transport vary substantially in magnitude, but all have small values in the summer hemisphere and large positive tendencies in the winter. The peak in the tendency of H_2O due to diffusive transport occurs in mid-latitudes in the winter hemisphere. The peak magnitudes of H_2O tendency due to diffusive transport are 14, 56, and 91 ppb day⁻¹ for Prandtl numbers of 100, 10, and 1 respectively. These relative magnitudes indicate that the negative feedback of vertical structure on the transport is having an effect. Rather than a factor of 10 increase in diffusive tendency with decreasing Prandtl number, as would occur without feedback, the increases are only factors of 2-4.

Significant differences occur in the mean advection contributions to H_2O tendency in the three cases. In the

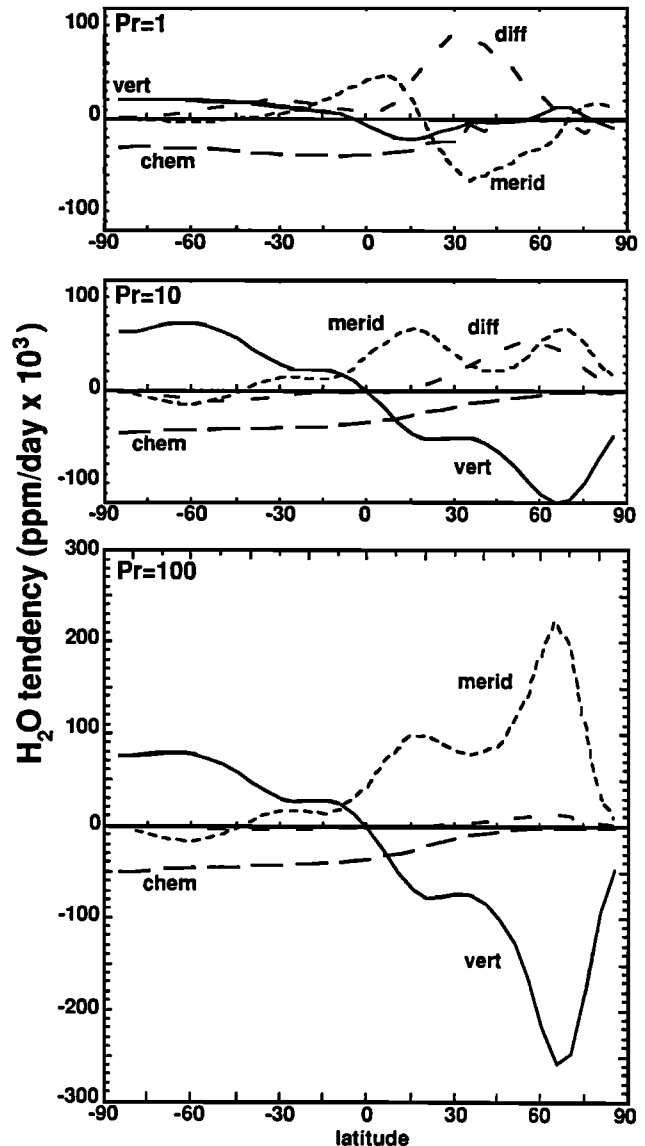


Fig. 3. Relative magnitude of processes tending to change the H_2O mixing ratio, averaged over the height range 70-80 km for the month of January. Frames correspond to the model runs with $Pr=1$ (top), $Pr=10$ (center), and $Pr=100$ (bottom). Curves shown are vertical advection by the mean circulation (vert), meridional advection by the mean circulation (merid), photochemical production and loss (chem), and vertical diffusive transport (diff).

$Pr=100$ case, the magnitude of the removal by vertical advection is large, which is consistent with a steep negative gradient in the water mixing ratio. In the $Pr=10$ case, vertical advection tends to cause a transport of H_2O into the summer hemisphere that is comparable to the $Pr=100$ case, and a weaker, but still dominant, removal of water from the winter hemisphere. In the case with highest diffusion ($Pr=1$), the tendencies due to vertical advection are smaller in both hemispheres and virtually disappear in the winter hemisphere. Meridional advection is tending to increase the H_2O concentration in all except high southern latitudes in the two higher Prandtl number cases but removes H_2O from the winter hemisphere in the $Pr=1$ case. Since \bar{v}^* and \bar{w}^* are similar in the two model runs, the differences in the H_2O advective tendencies are almost entirely a result of differences in the H_2O concentrations.

The overall balance in the H₂O mixing ratio is summarized here.

In the summer hemisphere, photochemical loss is balanced primarily by H₂O increase due to transport, dominated by mean vertical advection.

In low latitudes, photochemical loss is offset primarily by the increase due to meridional advection, indicating a transport of higher H₂O air from the summer toward the winter hemispheres. Vertical advection by the mean circulation also plays a role.

In the winter hemisphere, photochemistry is very weak; a balance is attained between two or three of the transport processes. In the $Pr=1$ (high diffusion) case, the increase due to diffusion is offset by a decrease from meridional advection; vertical advection is small. In the cases with lower effective diffusion ($Pr=10$, $Pr=100$), vertical advection is tending to remove water vapor; this is balanced by increases resulting from meridional advection and, when $Pr=10$, by vertical diffusion.

The relative magnitudes of the tendencies due to diffusion in the three cases, noted above, indicates that the negative feedback is acting to generate weaker vertical gradients in H₂O when the effective diffusion is larger. Figure 4 shows the model generated value of H₂O scale height, determined from $h_s = \bar{\mu} (\partial \bar{\mu} / \partial z)^{-1}$, for the three model runs. For the $Pr=10$ and $Pr=100$ runs, the model h_s is very large in the lower mesosphere, reflecting the very weak vertical gradient there, and is quite small at the mesopause where photochemistry is inducing a rapid decrease of mixing ratio with height. There is a large variation of h_s with height in the lower mesosphere, which means that (6) is not strictly accurate (the assumption that vertical derivatives of h_s are negligible is implicit in the derivation). When the effective diffusion rate is high ($Pr=1$), the vertical scale height in the upper mesosphere is much larger, indicating that rapid vertical mixing is taking place. In the upper mesosphere (75–80 km) the reductions of h_s with each tenfold increase in Prandtl number are as large as, or larger

than, the $\sqrt{10}$ reduction expected from the feedback in (4), indicating that even with a weak vertical diffusion coefficient the negative feedback between the effective vertical diffusion coefficient and the scale height is strong enough to have a significant impact on the ensuing structure of water vapor.

Monthly average observations of the seasonal cycle of H₂O at 40°N were presented by *Bevilacqua et al.* [1989]. Because of the weak signal from the upper mesosphere, resolution of the season cycle at 80 km from these data is near the measurement sensitivity limit, so some features of the distribution may not be resolved. Time-height cross sections of model simulations of water from the three model runs are given in Figure 5 for comparison with the data. Note that the model results are on constant log pressure surfaces, whereas the measurements are a function of altitude. The $Pr=1$ case does not compare well with the observations. Two features in particular differ substantially from the microwave observations when the model diffusion is large: the vertical gradient in the model upper mesosphere is very weak and there is a strong maximum of water vapor mixing ratio in late winter as well as late summer. Both of these discrepancies show a marked decrease when the effective diffusivity in the model is reduced. The differences between the $Pr=10$ and $Pr=100$ cases are less.

Differences can appear when data are viewed as a function of altitude, rather than log pressure, as noted by *Thomas* [1990]. Because temporal variations in K_{zz} enter into the heat budget, they tend to shift the height of pressure surfaces in phase with changes in the water vapor transport. Increased K_{zz} tends to cool, so a given altitude corresponds to a lower pressure, where, because of the negative gradient, H₂O is lower. This partially counteracts the other effect of increased K_{zz} , which, in the mesosphere, is to increase the H₂O by upward transport. Therefore, variations of H₂O due to K_{zz} fluctuations are in general weaker on a constant altitude surface than on a nearby constant pressure surface.

Figure 6 shows time series of the water vapor at 40°N and 75 and 80 km altitude for comparison with the results of *Bevilacqua et al.* [1989, 1990]. In addition to the three runs discussed previously, the figure also shows results from a case with $Pr=3$ and a case where K_{zz} was a function of latitude and height but was held constant in time at the average of the $Pr=10$ case. In the fixed K_{zz} case, the wave drag, used to determine the momentum balance, was allowed to vary as before but was decoupled from the diffusivity. At both altitudes a smooth transition from a dominant semiannual cycle ($Pr=1$) to a dominant annual cycle ($Pr=100$) with decreasing diffusivity is clearly evident. The H₂O mixing ratio is substantially higher for the large diffusion case. At and below 70 km in the lower mesosphere this is reversed (not shown), and the lower diffusion cases have slightly larger mixing ratio values. At 75 km the average mixing ratios are larger than observed during the partial-year span of microwave operation. (Average values at 75 km are not given by *Bevilacqua et al.* [1989], but contour plots indicate that the values range from lows of 1.5–2 ppmv to highs of 3.5–4 ppmv.) At 80 km there is better correspondence between the model and the observations for the cases with Prandtl numbers of 3 or more. The winter/spring values presented by *Bevilacqua et al.* [1990], ranging between 0.5 and 2 ppmv, are within the range spanned by the $Pr=3$, $Pr=10$, and $Pr=100$ model cases.

Agreement in the timing of the variation is more difficult to assess because of large gaps in the microwave data record. If the single point given by *Bevilacqua et al.* [1990] for

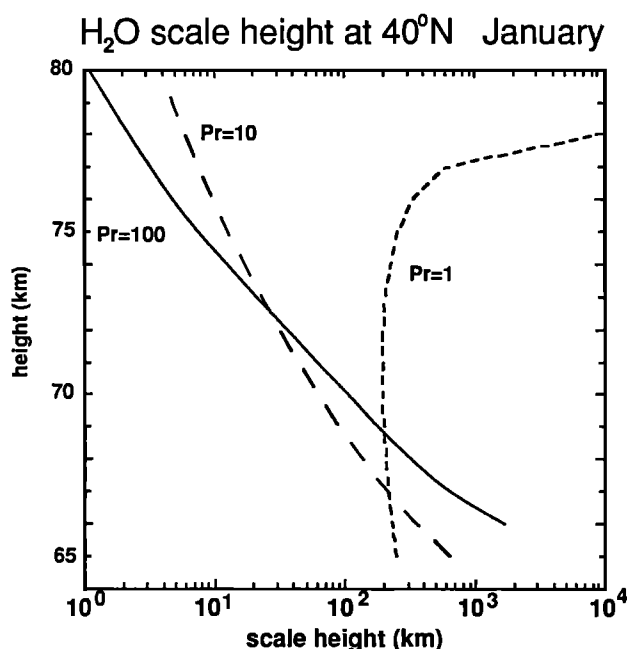


Fig. 4. The scale height (in kilometers) of H₂O in the mesosphere, averaged over the month of January, for the three model runs.

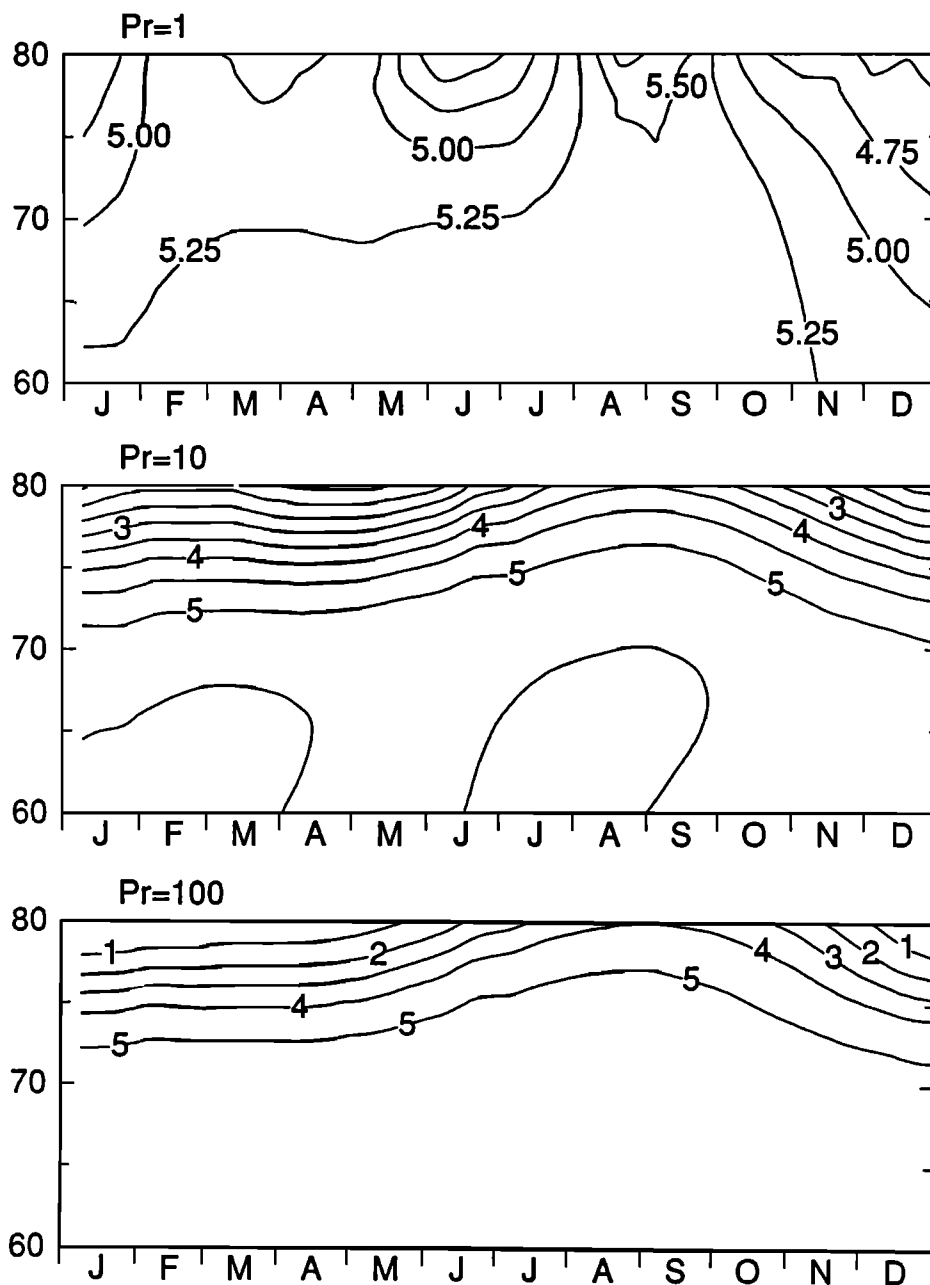


Fig. 5. H_2O mixing ratio (ppmv) for the model runs with $Pr=1$ (top), $Pr=10$ (center), and $Pr=100$ (bottom), plotted versus model vertical coordinate (approximate height) and time for one model year at 40°N . Contour interval is 0.25 ppmv for the top panel, 0.5 ppmv for the center panel, and 1 for the bottom panel.

September (their Figure 3) from data at Haystack is representative, it would indicate that the peak in H_2O mixing ratio in all the present model runs occurs too late and is too large. In addition, the model runs with Prandtl numbers of 3 and 10 indicate a secondary maximum in water mixing ratio in late winter that does not occur in the observations. The $Pr=100$ run does not have this maximum, but has extremely small H_2O mixing ratios during winter and spring. Because of this, the best match with the observations occurs for the fixed K_{zz} case, which is also lacking the late winter maximum. (The consistently lower H_2O mixing ratios from the $Pr=10$ case, as compared with those from the run with fixed K_{zz} , are a result of the negative correlation in time between the magnitude of K_{zz} and the strength of the water vapor vertical gradient.)

Several other studies have presented profiles of H_2O in the mesosphere obtained from other techniques [Kopp, 1990; Grossmann *et al.*, 1985, 1987; Arnold and Krankowsky, 1977; Laurent *et al.*, 1986]. The range of values between these soundings is much greater than that which would be expected from the ground-based Jet Propulsion Laboratory and Penn State [Bevilacqua *et al.* 1989] data. Several of the high-latitude soundings [Kopp, 1990; Grossmann *et al.*, 1985; 1987; Arnold and Krankowsky, 1977] have very weak negative, or even positive vertical mixing ratio gradients, which would agree most closely to the low Prandtl run of the two-dimensional model. (If there is indeed an increase in H_2O with height in the global mean over an extensive region and period of time, there must be an important photochemical source or physical

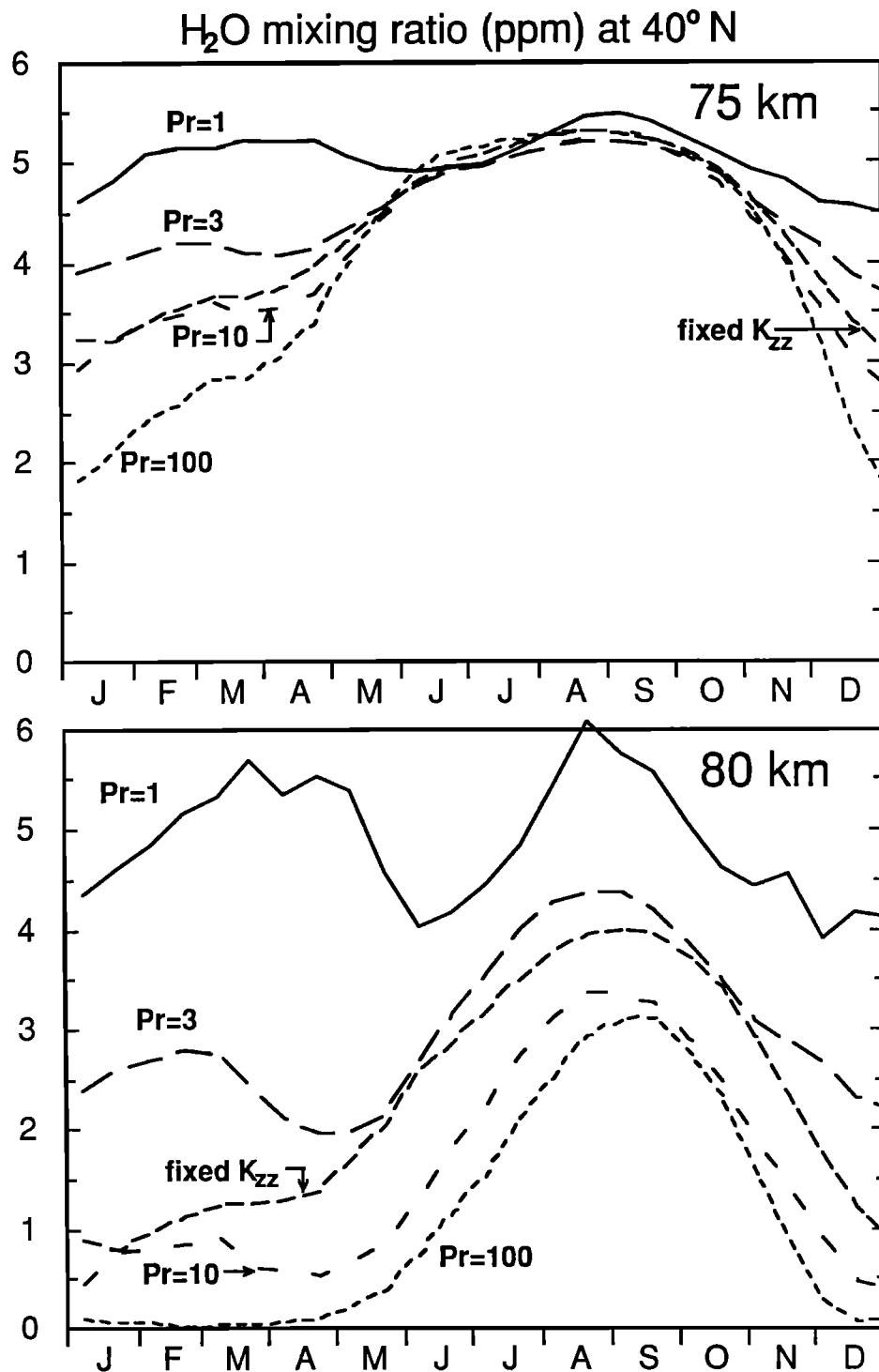


Fig. 6. H_2O mixing ratio (ppmv) for one model year at 40°N and 75 (upper) and 80 (lower) km altitude from five model runs.

process, such as molecular diffusion, that is not considered in these model studies.) There are also several examples showing a very sharp negative gradient in middle [Laurent *et al.*, 1986] or high [Kopp, 1990] latitudes, which are more consistent with the highest Prandtl number model simulation. The error bars associated with the measurements can be almost as large as the variations themselves. If we assume that the data give an indication of the real variability of H_2O in the mesosphere,

then the collective set of water vapor soundings indicates that the variability in H_2O concentration can be substantial.

Because of the sparsity of the profiles, it is not possible to distinguish variability associated with the seasonal cycle from that on shorter time scales. With this range of concentrations, no single one of our model runs simulates all cases. We infer from the model results that substantial local or short-term changes in the effective diffusion, lasting at least as

long as the transport time for H₂O (~1 week), might be capable of giving strongly different profiles of H₂O. The individual profile data would indicate that the effective diffusion rate varies widely, at least in high northern latitudes, where the majority of profiles are located. The variability in vertical diffusivity could result from intermittency in the rate of gravity wave breaking or from variations in the effective Prandtl number under different conditions.

5. SUMMARY

The initial question motivating this study was whether diffusion or mean advection determined the distribution and seasonal variation of mesospheric water vapor. To address this, three runs of a two-dimensional numerical model were performed that were identical except that the effective Prandtl number varied over several orders of magnitude. From the analysis of these model runs we feel a need to reformulate the question somewhat. Diffusive transport was found to be closely tied to the vertical structure of water vapor, regardless of whether the effective diffusion was large or small (within the broad range investigated). Both the vertical structure and the seasonal variations are sensitive to the diffusion rate. This conclusion results from the strong feedback between the effective vertical diffusion coefficient and the vertical structure of water vapor. Both meridional and vertical advection by the mean meridional circulation were important in controlling the distribution. The relevant question is, then, which Prandtl number results in a more realistic distributions of water.

Two additional model runs were performed, one with $Pr=3$ and the other with K_{zz} held fixed in time, to round out the set of cases for direct comparison of the model with the accumulated set of microwave measurements. There is a clear indication from this study that the moderate Prandtl numbers ($Pr=3$ and $Pr=10$) result in vertical distributions and seasonal variations of water that correspond more closely to the midlatitude microwave measurements of mesospheric water presented recently by *Bevilacqua et al.* [1989] than do either of the extremes ($Pr=1$ and $Pr=100$). There also is an indication that the seasonal variability in the diffusivity, which is a direct outcome of using the Lindzen parameterization to calculate K_{zz} , actually diminishes the ability of the model to simulate the water distribution. These limited model studies suggest that, in the interest of simulating the water vapor distribution in the mesosphere observed by microwave sounders, moderate values of Prandtl number are preferable. Other measurement techniques [*Kopp*, 1990; *Grossmann et al.*, 1985, 1987; *Arnold and Krankowsky*, 1977; *Laurent et al.*, 1986] show a wide range of H₂O concentrations; individual profiles can be found whose vertical structures conform most closely to the high, moderate, or low Prandtl numbers simulations of the two-dimensional model.

The present results can be compared to those of *Garcia and Solomon* [1985] and *Holton and Schoeberl* [1988], which came to contradictory conclusions regarding the importance of diffusion in controlling the mesospheric water vapor budget. Like *Garcia and Solomon* [1985], we find a semiannual cycle in water vapor that is correlated with the semiannual cycle in vertical diffusion when we use the high diffusion derived from *Lindzen's* [1981] parameterization with $Pr=1$. This conclusion concerning the importance of diffusion differs from that reached by *Holton and Schoeberl* [1988], who found that the

seasonal variation of H₂O was controlled by vertical advection, and that variations in the effective Prandtl number did not have an impact on the simulated distribution of water. However, their model appears not to have included the strong dependence of the vertical structure of H₂O mixing ratio, represented by a scale height h_p , on the diffusion. It may be that their chemical scheme, with a linear relaxation to an equilibrium water vapor profile, constrains the vertical structure and is therefore responsible for their conclusion on the secondary role of diffusion. The present model studies with $Pr \geq 10$ support *Holton and Schoeberl's* [1988] overall finding that it is mean vertical advection, rather than vertical diffusion, that is more important in the budget of H₂O. The primary difference is that we find that diffusion is instrumental in determining the vertical structure of water, and that, even when the effective diffusion coefficient is small, its precise value can have an impact on the simulated H₂O distribution. Trace species distributions have been used in previous studies to deduce the vertical diffusion rate [e.g., *Allen et al.*, 1981; *Brasseur and Offermann*, 1986]; our conclusions hold out hope that this approach will be able to improve estimates of the magnitude and variability of mesospheric vertical diffusion as future trace species measurements become available.

Water vapor is the primary source of the odd hydrogen species that react with ozone in the mesosphere. *Thomas et al.* [1984] and *Garcia and Solomon* [1985] noted that the semiannual variation in H₂O would contribute to a semiannual variation in ozone, and that such ozone periodicity had been observed by SME. However, recent analyses of ground-based H₂O observations [*Bevilacqua et al.*, 1989] indicate that the semiannual component of the H₂O temporal variation is probably small. The seasonal evolution of water in our model more closely resembles that found by the microwave observations when the effective vertical diffusion rate is reduced by using a Prandtl number of 10 or more. A factor of 10 reduction in the vertical diffusion is consistent with recent theoretical estimates that indicate that the effective Prandtl number in the mesosphere is significantly greater than one. When the semiannual periodicity in mesospheric water is reduced in the model, much of the semiannual periodicity of odd oxygen [O+O₃+O(¹D)] disappears also and an anticorrelation in time between water and odd oxygen is evident. *Thomas* [1990] discussed a mechanism that can account for the observed ozone temporal variability without a similar variation in the total odd oxygen, which is dominated by atomic oxygen near the mesopause. He demonstrated that a semiannual variation in ozone can result from the product of two annual terms: one term is the annual cycle in odd oxygen and the other is the variation in the partitioning between O and O₃ due to variability in the chemical composition (particularly, atomic hydrogen), solar insolation and the dependence of chemical reaction rates on temperature. In our model the ozone variability at 80 km is closely correlated with the total odd oxygen amount and, for moderate values of Prandtl number, has only a weak semiannual variability which is anticorrelated with that of water. With these model studies we are not able to reconcile the pronounced semiannual variability in ozone in the mesosphere measured by SME with the predominantly annual periodicity of water detected by ground-based microwave sounders.

Acknowledgments. We thank R. Garcia and M. Schoeberl for comments on an earlier version of this paper. This work has been supported by National Science Foundation grant ATM-8808562.

Computing funds were provided by National Center for Atmospheric Research (NCAR). NCAR is sponsored by the National Science Foundation.

REFERENCES

- Allen, M., Y. L. Yung, and J. W. Waters, Vertical transport and photochemistry in the terrestrial mesosphere and lower thermosphere (50-120 km), *J. Geophys. Res.*, **86**, 3617-3627, 1981.
- Andrews, D. G., and M. E. McIntyre, Planetary waves in horizontal and vertical shear: The generalized Eliassen-Palm relation and the mean zonal acceleration, *J. Atmos. Sci.*, **33**, 2031-2048, 1976.
- Arnold, F., and D. Krankowsky, Water vapour concentrations at the mesopause, *Nature*, **268**, 218-219, 1977.
- Bevilacqua, R. M., J. J. Olivero, and C. L. Croskey, Mesospheric water vapor measurements from Penn State: Monthly mean observations (1984-1987), *J. Geophys. Res.*, **94**, 12,807-12, 818, 1989.
- Bevilacqua, R. M., D. F. Strobel, M. E. Summers, J. J. Olivero, and M. Allen, The seasonal variation of water vapor and ozone in the upper mesosphere: Implications for vertical transport and ozone photochemistry, *J. Geophys. Res.*, **95**, 883-893, 1990.
- Brasseur, G., and M. H. Hitchman, The effect of breaking gravity waves on the distribution of trace species in the middle atmosphere, in *Transport Processes in the Middle Atmosphere*, edited by G. Visconti and R. Garcia, D. Reidel, Hingham, Mass., 1987.
- Brasseur, G., and D. Offermann, Recombination of atomic oxygen near the mesopause: Interpretation of rocket data, *J. Geophys. Res.*, **91**, 10,818-10,824, 1986.
- Brasseur, G., M. H. Hitchman, S. Walters, M. Dymek, E. Falise, and M. Pirre, An interactive chemical dynamical radiative two-dimensional model of the middle atmosphere, *J. Geophys. Res.*, **95**, 5639-5655, 1990.
- Chao, W. C., and M. R. Schoeberl, On the linear approximation of gravity wave saturation in the mesosphere, *J. Atmos. Sci.*, **41**, 1893-1898, 1984.
- Coy, L., and D. C. Fritts, Gravity wave heat fluxes: A Lagrangian approach, *J. Atmos. Sci.*, **45**, 1770-1780, 1988.
- DeMore, W. B., M. J. Molina, S. P. Sander, D. M. Golden, R. F. Hampson, M. J. Kurylo, C. J. Howard, and A. R. Ravishankara, Chemical kinetics and photochemical data for use in stratospheric modeling, *JPL Publ.*, **87-41**, 196, 1987.
- Fritts, D. C., and T. J. Dunkerton, Fluxes of heat and momentum due to convectively unstable gravity waves, *J. Atmos. Sci.*, **42**, 549-556, 1985.
- Garcia, R. R., Dynamics, radiation and photochemistry in the mesosphere: Implications for the formation of noctilucent clouds, *J. Geophys. Res.*, **94**, 14, 605-14,615, 1989.
- Garcia, R. R., and S. Solomon, The effect of breaking gravity waves on the dynamics and chemical composition of the mesosphere and lower thermosphere, *J. Geophys. Res.*, **90**, 3850-3868, 1985.
- Gille, J. C., and J. M. Russell III, The Limb Infrared Monitor of the Stratosphere: Experiment description, performance and results, *J. Geophys. Res.*, **89**, 5125-5140, 1984.
- Grossmann, K. U., W. G. Frings, D. Offermann, L. André, E. Kopp, and D. Krankowsky, Concentrations of H₂O and NO in the mesosphere and lower thermosphere at high latitudes, *J. Atmos. Terr. Phys.*, **47**, 291-300, 1985.
- Grossmann, K. U., W. G. Frings, D. Offermann, L. André, E. Kopp, and D. Krankowsky, Middle atmosphere abundances of water vapor and ozone during MAP/WINE, *J. Atmos. Terr. Phys.*, **49**, 827-841, 1987.
- Hitchman, M. H., and G. Brasseur, Rossby wave activity in a 2-D model: Closure for wave driving and meridional eddy diffusivity, *J. Geophys. Res.*, **93**, 9405-9417, 1988.
- Holton, J. R., and M. R. Schoeberl, The role of gravity wave generated advection and diffusion in transport of tracers in the mesosphere, *J. Geophys. Res.*, **93**, 11,075-11, 082, 1988.
- Jones, R. L., J. A. Pyle, J. E. Harries, A. M. Zavody, J. M. Russell, and J. C. Gille, The water vapor budget of the stratosphere studied using LIMS and SAMS satellite data, *Q. J. R. Meteorol. Soc.*, **112**, 1127-1143, 1986.
- Keyser, L. F., K. Y. Choo, and M. T. Leu, Yields of O₂ ($b^1\Sigma_g^+$) from reactions with HO₂, *Int. J. Chem. Kinet.*, **17**, 1169-1185, 1985.
- Kiehl, J. T., R. J. Wolski, B. P. Briegleb, and V. Ramanathan, Documentation of radiation and cloud routines in the NCAR community climate model (CCM1), *Tech. Note NCAR/TN-288+IA*, Natl. Cent. for Atmos. Res., Boulder, CO., 1987.
- Kopp, E., Hydrogen constituents of the mesosphere inferred from positive ions: H₂O, CH₄, H₂CO, H₂O₂ and HCN, *J. Geophys. Res.*, **95**, 5613-5630, 1990.
- Laurent, J., D. Brard, A. Girard, C. Camy-Peyret, C. Lippens, C. Müller, J. Vercheval, and M. Ackerman, Middle atmospheric water vapor observed by Spacelab One grille spectrometer, *Planet. Space Sci.*, **34**, 1067-1071, 1986.
- Le Texier, H., S. Solomon, and R. R. Garcia, The role of molecular hydrogen and methane oxidation in the water vapour budget of the stratosphere, *Q. J. R. Meteorol. Soc.*, **114**, 281-295, 1988.
- Lindzen, R. S., Turbulence and stress owing to gravity wave and tidal breakdown, *J. Geophys. Res.*, **86**, 9707-9714, 1981.
- Nicolet, M., Etude des réactions chimiques de l'ozone dans la stratosphère, Institut Royal Météorologique de Belgique, Brussels, Belgium, 1978.
- Nicolet, M., Aeronomic chemistry of ozone, *Planet. Space Sci.*, **37**, 1621-1652, 1989.
- Randel, W. J., Global Atmospheric Circulation Statistics, 1000-1 mb, *Tech. Note NCAR/TN-295+STR*, Natl. Cent. for Atmos. Res., Boulder, CO., 1987.
- Schoeberl, M. R., A model of gravity wave breakdown with convective adjustment, *J. Atmos. Sci.*, **45**, 980-992, 1988.
- Strobel, D. F., J. P. Apruzese, and M. R. Schoeberl, Energy balance constraints on gravity wave induced eddy diffusion in the mesosphere and lower thermosphere, *J. Geophys. Res.*, **90**, 13,067-13,072, 1985.
- Strobel, D. F., M. E. Summers, R. M. Bevilacqua, M. T. DeLand, and M. Allen, Vertical constituent transport in the mesosphere, *J. Geophys. Res.*, **92**, 6691-6698, 1987.
- Thomas, R. J., Atomic hydrogen and atomic oxygen density in the mesopause region: Global and seasonal variations deduced from Solar Mesosphere Explorer near-infrared emissions, *J. Geophys. Res.*, **95**, 16,457-16,476, 1990.
- Thomas, R. J., C. A. Barth, and S. Solomon, Seasonal variations of ozone in the upper mesosphere and gravity waves, *Geophys. Res. Lett.*, **11**, 673-676, 1984.

G. Brasseur, National Center for Atmospheric Research, P.O. Box 3000, Boulder, CO 80307.
A. K. Smith, Space Physics Research Laboratory, Department of Atmospheric, Oceanic and Space Sciences, University of Michigan, Ann Arbor, MI 48109.

(Received July 5, 1990;
revised January 16, 1991;
accepted January 16, 1991)